

Spatial System Identification of a Simply Supported Beam and a Trapezoidal Cantilever Plate.

A. Fleming¹

S. O. R. Moheimani¹

Abstract

Dynamic models of structural and acoustic systems are usually obtained by means of modal analysis or finite element modelling. To their detriment, both techniques rely on a comprehensive knowledge of the system's physical properties. Experimental data and a non-linear optimization is often required to refine the model. For the purpose of control, system identification is often employed to estimate the dynamics from disturbance and command inputs to a set of outputs. Such discretization of a spatially distributed system places further unknown weightings on the control objective, in many cases, contradicting the original goal of optimal control. This paper introduces a frequency domain system identification technique aimed at obtaining spatially continuous models for a class of distributed parameter systems. The technique is demonstrated by identifying a simply supported beam and trapezoidal cantilever plate, both with bonded piezoelectric transducers. The plate's dimensions are based on the scaled front elevation of a McDonnell Douglas FA-18 vertical stabilizer¹.

1 Introduction

In the analysis and control of distributed parameter systems it is of great benefit to possess a spatial model. That is, a model that describes system dynamics over an entire spatial domain. This paper is concerned with the modelling and identification for a class of distributed parameter systems. Such systems include but are not limited to: flexible beams and plates, compound linear structures, slewing structures, and acoustic enclosures.

The motivation for finding such a model lies in both the fields of analysis and synthesis. During analysis the user may simply wish to observe the mode shapes of the structure, or in a more complete utilization of the model, mathematically estimate the spatial feedback control performance of a system utilizing discrete sensors, actuators, and control objectives. For example, consider [1] where a standard H_∞ controller [2, 3] is designed to minimize vibration at a single point on a piezoelectric laminate simply supported beam. A spatial model is required to analyze the overall performance of such a controller. The fact that the point-wise controller is shown to provide good local performance but poor spatial performance leads us to the primary application of spatial models - spatial controller synthesis. A number of standard control synthesis variants have emerged that address the control design of spatially distributed systems with discrete sensors and actuators. Recent examples include: spatial feed-forward

control [4], spatial resonant control [5], spatial H_2 control [6], and spatial H_∞ control [1].

The modal analysis procedure has been used extensively throughout the literature for obtaining spatial models of structural [7, 8] and acoustic systems [9]. Its major disadvantage being the requirement for detailed physical information about the sensors, actuators, and underlying system. Practical application typically involves the use of experimental data and a non-linear optimization to identify unknown parameters such as modal amplitudes, resonant frequencies, and damping ratios. Even in this case the descriptive partial differential equations must still be solved (as functions of the unknown parameters) to obtain the mode shapes. This may be difficult or impossible for realistic structural or acoustic systems with complicated boundary conditions.

Another popular technique for obtaining spatial models is that of finite element (FE) analysis [10]. This is an approximate method that results in high order spatially discrete models. If the dynamics of sensors and actuators are known, the integrated model can be cast in a state space form to facilitate control design and analysis [11]. The approximate nature of finite element modelling eliminates the need for solving descriptive partial differential equations. Detailed information relating to the structure's material properties and boundary conditions is still required. As with the modal analysis procedure, FE models are usually tuned with experimental data [12].

A considerable literature has also developed on the topic of *Experimental Modal Analysis*, (see [13] for a compilation of such methods). These methods can be predominantly described as frequency domain transfer function methods. The system is assumed to consist solely of parallel second order resonant sections. Sensor, actuator, and additional non-modal dynamics are neglected. One of the most popular methods, widely used in commercial frequency domain modal analysis packages, is the rational fraction polynomial method [13]. As a transfer function method, the model is poorly conditioned, incorrectly describes the systems zero dynamics [14], and neglects non-modal dynamics. In addition, all of the mentioned experimental modal analysis techniques neglect the fundamental limitations in spatial sampling, i.e. Reconstructed mode shapes can be distorted due to violation of the Nyquist criterion in one or two dimensions.

This paper introduces an efficient and correct method for identifying the above class of systems directly from measured frequency response data.

¹School of Electrical Engineering and Computer Science, University of Newcastle, Australia. e-mail: andrew@ee.newcastle.edu.au

1.1 Modelling

The Lagrangian/modal expansion, or Ritz-Kantorovitch method [7] is commonly used to express the spatial deflection of a distributed parameter system as an infinite summation of modes. As discussed in [7] the model can be expressed in the frequency domain.

$$G_y(s, \mathbf{p}) = \sum_{i=1}^{\infty} \frac{F_i \phi_i(\mathbf{p})}{s^2 + 2\zeta_i \omega_i s + \omega_i^2} \quad (1)$$

$G_y(s, \mathbf{p})$ is the transfer function from an external force, or for the system considered in this paper, the piezoelectric voltage, to the displacement at a point \mathbf{p} , a coordinate vector on the spatial domain \mathcal{R} . The $\phi_i(\mathbf{p})$'s are the system eigenfunctions and must form a complete coordinate basis for the system, satisfy the geometric boundary conditions, and for analytic analysis be differentiable over the spatial domain to at least the degree required by the describing partial differential equations. Many practical systems also obey certain orthogonality conditions. ζ_i and ω_i are the damping ratios and resonance frequencies of each mode $\phi_i(\mathbf{p})$.

For practical reasons, (1) is often truncated to include only a certain number of modes that approximate the response over a limited bandwidth. Reference [14] introduces a model reduction technique for systems that satisfy certain modal orthogonality conditions. We define the model of a general single input spatially distributed system as,

$$\hat{G}_y(\mathbf{p}, s) = H(s) \left[\sum_{i=1}^N \frac{\Phi_i(\mathbf{p})}{s^2 + 2\zeta_i \omega_i s + \omega_i^2} + D(\mathbf{p}) \right] \quad (2)$$

where, $H(s)$ is the concatenation of all non-distributed transfer functions, $\Phi_i(\mathbf{p})$ is the i^{th} mode shape, and $D(\mathbf{p})$ is the feed-through function included to compensate for all higher order truncated contributions to zero dynamics. The filter $H(s)$ is used to model the additional dynamics of sensors, actuators, and for example, anti-aliasing filters. In this work $H(s)$ is not identified automatically.

The system (2) has a corresponding state space representation.

$$\begin{aligned} \dot{\mathbf{x}}(t) &= \mathbf{A}\mathbf{x}(t) + \mathbf{B}u(t) \\ d(\mathbf{p}, t) &= \mathbf{C}_Y(\mathbf{p})\mathbf{x}(t) + D_y(\mathbf{p})u(t) \end{aligned} \quad (3)$$

where, $\mathbf{C}_Y(x) = [\Phi_1(\mathbf{p}) \ 0 \ \dots \ \Phi_N(\mathbf{p}) \ 0]$, $\mathbf{B} = [0 \ 1 \ \dots \ 0 \ 1]^T$, N is the number of modes to be identified, and

$$\mathbf{A} = \begin{bmatrix} 0 & 1 & 0 & 0 \\ -\omega_1^2 & -2\zeta_1\omega_1 & 0 & 0 \\ & & \ddots & \\ 0 & 0 & 0 & 1 \\ 0 & 0 & -\omega_N^2 & -2\zeta_N\omega_N \end{bmatrix} \in \mathbf{R}^{2N \times 2N} \quad (4)$$

2 Spatial Sampling

Consider the model structure (2), the spatial functions $\Phi_i(\mathbf{p})$ and $D(\mathbf{p})$ must be reconstructed from their iden-

tified samples. For a uniformly sampled one dimensional system,

$$\begin{aligned} \Phi_i(\mathbf{p}_n) \\ D(\mathbf{p}_n) \end{aligned} = \begin{aligned} \Phi_i(\mathbf{p}) \\ D(\mathbf{p}) \end{aligned} \Big|_{\mathbf{p}=\mathbf{p}_n} \quad \begin{aligned} \mathbf{p}_n = n \Delta x \in \mathcal{R} \\ n \in \{0, 1, \dots, N_p\} \end{aligned} ,$$

there are a number of options available for reconstructing the continuous functions. Two of which are, traditional linear reconstruction, and spline reconstruction. The aim of this section is to quantify the expected mean square difference between the original continuous function and its corresponding reconstruction. This will allow us to evaluate the required spatial sampling interval as a function of the permissible error. An example of this procedure is performed for a simply supported beam in Section 2.1.

In general, a spatial function $f(x)$ will not be band-limited. Examples include, the mode shapes of a cantilever beam [8], and the feed-through function for a simply supported beam [14]. Since the samples are obtained indirectly from point-wise frequency response data, no form of low pass filtering is possible.

In recent years, splines have been recognized for their usefulness in curve and surface fitting problems [15], [16]. The function $f(x)$ can be approximately reconstructed from a spline basis $\varphi(x)$, with coefficients $c(k)$ derived from $f(k\Delta x)$.

$$Q^{sp} f(x) = \sum_{k \in \mathcal{Z}} c(k) \varphi^n\left(\frac{x}{\Delta x} - k\right) \quad (5)$$

where, $c(k) \in l_2$ are the (finite square summable)

spline coefficients, $Q^{sp} f(x)$ is the spline reconstruction of $f(x)$, and $\varphi^n(x)$ is the spline generating function. We will limit our choice of generating functions to the $(n+1)^{\text{th}}$ order β -splines (degree n) [16]. The condition

$c(k) \in l_2$ ensures that $Q^{sp} f(x)$ is a well defined subspace of L_2 , a considerably larger space than the traditional Shannon space of band limited functions. References [17] and [18] present a unified sampling theory for a wide class of interpolating functions. In likeness to the Shannon sampling theorem, the optimal spline reconstruction involves an optimal prefiltering before sampling and reconstruction by the chosen spline basis. The results in this area, including expressions for the RMS error, are summarized in [16]. In our application where a least squares fit is sought, the method of quantitative fourier analysis is easily applied to quantify the RMS reconstruction error [19]. The sampling phase averaged error is given by,

$$Er = \left[\frac{1}{2\pi} \int_{-\infty}^{\infty} |F(j\omega_x)|^2 E^n(\Delta x \omega_x) d\omega_x \right]^{\frac{1}{2}} \quad (6)$$

where $Er = \left\| f(x) - Q^{sh} f(x) \right\|_2$, and $E^n(\Delta x \omega_x)$ is defined as the frequency error kernel and is a function of the interpolant and Δx . Analytic expressions for $E^n(\Delta x \omega_x)$ have been given for the β -splines of order up to 6 [19].

2.1 Sampling of a Simply Supported Beam

This section demonstrates how the previous results can be applied to spatial systems. We present an example analysis for a simply supported beam. The objective is to arrive at a point where Equation (6) can be applied. Both expressions require only power spectral density of the function.

The mode shapes of a simply supported beam are given in [7], $\phi_i(x) = \sqrt{\frac{2}{\rho A_r L}} \sin\left(\frac{i\pi x}{L}\right) = \alpha \sin\left(\frac{i\pi x}{L}\right)$, where ρ is the material density, A_r is the cross-sectional area, and L is the length of the beam. The spatial spectra of $\sum_{i=1}^N \phi_i(x)$ is impulsive and easily determined,

$$F\left\{\sum_{i=1}^N \phi_i(x)\right\} = j\pi\alpha \sum_{i=1}^N \left[\delta(\omega_x + \frac{i\pi}{L}) - \delta(\omega_x - \frac{i\pi}{L})\right]. \quad (7)$$

The highest frequency component of $\phi_i(x)$ $i \in \{1, \dots, N\}$ is $\frac{N\pi}{L}$, thus, if we were to apply Shannon's Theorem² to reconstruct N mode shapes of a simply supported beam, $\frac{2\pi}{\Delta x} > 2\frac{N\pi}{L}$, that is, $\Delta x < \frac{L}{N}$. This simple and complete result applies in general to a subclass of the systems (1). Such systems are referred to as having *periodic* boundary conditions and are characterized by sinusoidal mode shapes.

The feed-through function $D(x)$ can be found analytically for systems of the form (1), $D(x) = \sum_{i=N+1}^{\infty} k_i \phi_i(x)$, where k_i is given in [14] as $k_i = \frac{F_i}{2\omega_c \omega_i} \ln\left(\frac{\omega_i + \omega_c}{\omega_i - \omega_c}\right)$. In order to find the power spectral density $|\mathcal{F}\{D(x)\}|^2$, it may be simpler to make a change of basis from the signal subspace spanned by $\phi_i(x)$ $i \in \{N+1, \dots, \infty\}$, to an enveloping subspace spanned by a set of functions with a known Fourier transform. In our case where $\phi_i(x)$ is sinusoidal, the following transformation is useful. By simply considering the Fourier series representation, $D(x) = \sum_{i \in \mathbb{Z}} c_i e^{i\frac{2\pi i x}{T_x}}$ where $T_x = 2L$,

$$c_i = \begin{cases} \frac{j}{2} \alpha \frac{F_i}{2\omega_c \omega_i} \ln\left(\frac{\omega_i + \omega_c}{\omega_i - \omega_c}\right) & i \in \{\dots, -N-1\} \\ 0 & i \in \{-N, \dots, N\} \\ -\frac{j}{2} \alpha \frac{F_i}{2\omega_c \omega_i} \ln\left(\frac{\omega_i + \omega_c}{\omega_i - \omega_c}\right) & i \in \{N+1, \dots\} \end{cases}. \quad (8)$$

The complex coefficients c_i reveal the spatial Fourier transform of $D(x)$.

$$\mathcal{F}\{D(x)\} = \mathcal{F}\left\{\sum_{i=N+1}^{\infty} k_i \phi_i(x)\right\} = \sum_{i=-\infty}^{\infty} 2\pi c_i \delta(\omega_s - i\frac{\pi}{L}) \quad (9)$$

where $\omega_r = \frac{2\pi}{T_x} = \frac{\pi}{L}$. As $\mathcal{F}\{D(x)\}$ does not have compact support on the interval $(-j\infty, j\infty)$, $D(x)$ can not be exactly reconstructed with any finite number of samples. It is also obvious from (9) that the spectra of $D(x)$ lies completely outside the bandwidth of the mode shapes, thus dictating the spatial sampling requirements of the system. We can now apply Equation (6) to determine the required spatial sampling

²Neglecting all other errors such as those resulting from truncation.

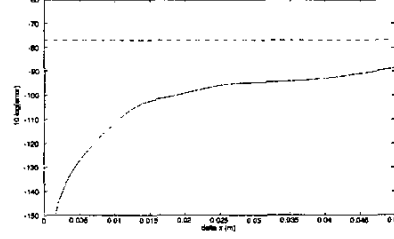


Figure 1: The RMS reconstruction error.

interval. For a periodic signal $g(t)$, the energy density per unit frequency is given in [20], $|G(f)|^2 = T_1 \sum_{n \in \mathbb{Z}} |c_n|^2 \delta(f - n\frac{1}{T_1})$, where T_1 is the period, $G(f)$ denotes the Fourier transform, and c_n are the Fourier coefficients of $g(t)$. By making a change of variables we can find the power spectral density of $D(x)$,

$$|\mathcal{F}\{D(x)\}|^2 = 2\pi T_x \sum_{i \in \mathbb{Z}} |c_i|^2 \delta(\omega_x - i\frac{2\pi}{T_x}). \quad (10)$$

Hence, from equation (6), the error in reconstructing $D(x)$ from an n^{th} order spline basis,

$$\|D(x) - D_{sp}^n(x)\|_2 = \left[2L \sum_{i \in \mathbb{Z}} |c_i|^2 E^n(i\pi \frac{\Delta x}{L})\right]^{\frac{1}{2}} \quad (11)$$

where $D_{sp}^n(x)$ is the spline reconstruction of $D(x)$. The error kernel for a cubic spline $E^4(i\pi \frac{\Delta x}{L})$ is plotted together with the equivalent Shannon kernel in [19]. We can also apply Parseval's equality to find the mean square value of $D(x)$ over one period, $\sum_{i=-\infty}^{\infty} |c_i|^2 = \frac{1}{2L} \int_{-L}^L |D(x)|^2 dx$.

We now consider a specific example: the simply supported beam described in Section 4, where 3 modes are retained for identification. In Figure 1 the RMS value of the reconstruction error (L_2 norm on $[-L, L]$) is plotted against the sampling interval Δx . As expected, as the sampling interval becomes large, the RMS error approaches the RMS value of the continuous function³. This plot can be used to select a spatial sampling interval that achieves some error specification on $D(x)$.

In summary, the sampling limitations for a simply supported beam have been derived. Even when the mode shapes are known *a priori*, this analysis can be difficult to perform. For the practitioner, we offer a rough rule of thumb. 1) Estimate, by means of a similar system or finite element analysis, the highest significant spatial frequency component of the highest order mode to be identified. 2) Consider the feed-through function $D(\mathbf{p})$. Assume that its highest significant frequency

³In this analysis we have considered $D(x) \notin L_2$. When we refer to the RMS or mean square value of such signals, we are implicitly referring to the RMS or mean square value over a single period.

component is three times that estimated in step 1). (This step is suggested on the experience of studying and identifying a number of such systems). 3) Sample the structure as would be done in practice for a function with spatial bandwidth derived in step 2). Taking into consideration the limited domain of the structure, (allowing for truncation errors), this would normally be between 2 to 5 times the rate suggested by the Nyquist criterion.

3 Identification

The first step in the identification procedure is to obtain an estimate for \mathbf{A} , the system matrix whose eigenvalues reveal the parallel dynamics of each mode. On first inspection, this problem may appear trivial as the transfer function obtained from a single frequency response would perform the task. For spatially distributed systems we must redefine our measures of model quality and stochastic performance. In essence, the two main sources of error in the identification arise from measurement noise and slight changes in system dynamics over the spatial domain. Intuitively, we would like to distribute the resulting model error in a similar, equally distributed fashion. The task of quantifying such errors is the subject of current research.

The problem can be cast as a MIMO system identification problem where each point is regarded as a single output. Subspace based algorithms have proven particularly useful for identifying high order multi-variable resonant systems [21]. The reader is referred to [22] and [23] for a full discussion of frequency domain subspace techniques.

3.1 Identifying the Mode Shapes and Feed-through Function

Samples of the spatial functions will now be identified from the available frequency response data. Some Definitions: \mathbf{G} , the spatial response matrix, \mathbf{P}^{tf} , the dynamic response matrix, Ψ , the modal function matrix, \mathbf{D} the feed-through vector.

$$\mathbf{G} = \begin{bmatrix} G(\mathbf{p}_1, j\omega_1) & \cdots & G(\mathbf{p}_{N_p}, j\omega_1) \\ \vdots & \ddots & \vdots \\ G(\mathbf{p}_1, j\omega_{N_\omega}) & \cdots & G(\mathbf{p}_{N_p}, j\omega_{N_\omega}) \end{bmatrix} \in \mathbf{C}^{N_\omega \times N_p} \quad (12)$$

$$\mathbf{P}^{tf} = \begin{bmatrix} P_1^{-1}(j\omega_1) & \cdots & P_N^{-1}(j\omega_1) \\ \vdots & \ddots & \vdots \\ P_1^{-1}(j\omega_{N_\omega}) & \cdots & P_N^{-1}(j\omega_{N_\omega}) \end{bmatrix} \in \mathbf{C}^{N_\omega \times N} \quad (13)$$

where $P_i^{-1}(j\omega)$ is the response of the ordered i^{th} mode dynamics found from the system matrix \mathbf{A} .

$$P_i^{-1}(j\omega) = \frac{1}{[s + (\alpha_i + j\sigma_i)][s + (\alpha_i - j\sigma_i)]} \Big|_{s=j\omega} \quad (14)$$

$$\Psi = \begin{bmatrix} \Phi_1(\mathbf{p}_1) & \cdots & \Phi_1(\mathbf{p}_{N_p}) \\ \vdots & \ddots & \vdots \\ \Phi_N(\mathbf{p}_1) & \cdots & \Phi_N(\mathbf{p}_{N_p}) \end{bmatrix} \in \mathbf{R}^{N \times N_p} \quad (15)$$

Frequency Range	10-200 (Hz)
Epi-distance F Samples	3031
Spatial Sampling interval	2.5 cm
Identification Samples	13
Validation Samples	13
Excitation	Colored Noise

Table 1: Identification Parameters

$$\mathbf{D} = [D(\mathbf{p}_1) \quad \cdots \quad D(\mathbf{p}_{N_p})] \in \mathbf{R}^{1 \times N_p} \quad (16)$$

We can form the following complex matrix equation

$$\mathbf{G} = [\mathbf{P} \quad \mathbf{1}_{N_\omega \times 1}] \begin{bmatrix} \hat{\Psi} \\ \hat{\mathbf{D}} \end{bmatrix} \quad (17)$$

Equation (17) has a unique least squares solution if $N_\omega \geq N$, this condition is automatically satisfied if the restrictions in Section 3 are met [23]. Since we are interested in real valued functions we restrict the matrices Ψ and $\hat{\mathbf{D}}$ accordingly.

For notational simplicity, we assume \mathbf{p} is single dimensional. Here the ordering and dimension of the co-ordinate vector \mathbf{p} becomes important. When using linear reconstruction, the spatial system can be written in state space form

$$\begin{aligned} \dot{\mathbf{x}} &= \mathbf{A}\mathbf{x} + \mathbf{B}u \\ Y(x) &= \mathbf{B}_r(x)^T \Psi^T J \mathbf{x} + \mathbf{D}\mathbf{B}_r(x)u \end{aligned} \quad (18)$$

where $\mathbf{B}_r(x)$ is the shannon reconstruction basis, and

$$J = \begin{bmatrix} e_1^T & e_3^T & \cdots & e_{(2N-1)}^T \end{bmatrix}^T \in \mathbf{R}^{N \times 2N}$$

The spline reconstructed system is similar to (18) except that the function samples $[\Psi \quad \mathbf{D}]^T$ and reconstruction basis \mathbf{B}_r are replaced by the spline coefficients and chosen basis.

4 Experimental Results

The presented technique will now be applied to identify two spatially distributed systems, a simply supported beam, and asymmetric cantilever plate. Both structures are excited using bonded piezoelectric actuators. Although the simply supported beam is easily modelled using analytic methods (albeit with experimental tuning), applying such techniques to the plate is significantly more difficult. The problem is complicated by the irregular geometry of the plate boundary.

Beam Identification: A photograph and physical parameters of interest can be found in [24]. Colored noise is applied to the actuator, the spatial response is measured sequentially using a Polytec scanning laser vibrometer. Details of the data set are given in Table 1.

The extracted mode and feed-through function samples together with their spline reconstructions is shown in Figure 2. To evaluate model quality, we will compare the spatial beam response plotted in Figure 3 (a), to the identified model response plotted in Figure 3 (b). The magnitude response of the error system is plotted in Figure 3 (c)

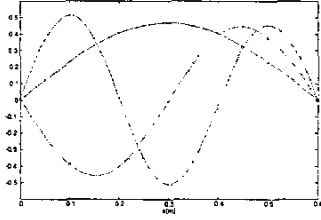


Figure 2: The extracted mode samples and spline reconstruction

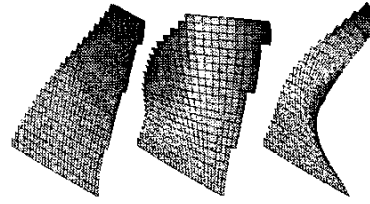


Figure 4: Identified fin modes.

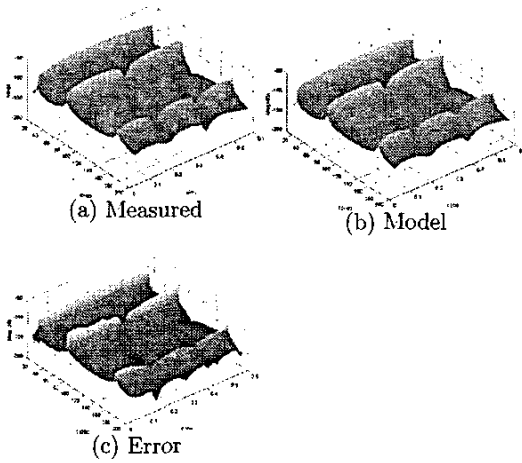


Figure 3:

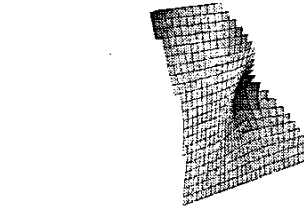


Figure 5: Identified feedthrough function.

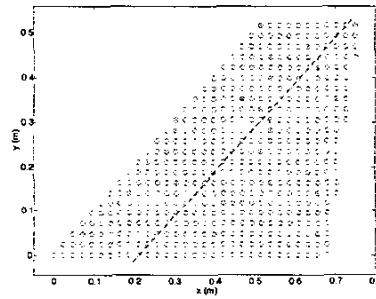


Figure 6: Distribution of the spatial samples. An 'x' represents the location of a sample used to identify the system matrix A . The dashed line represents the side elevation of a cross-section used to analyze model quality.

Plate Identification: The experimental plate is constructed from aluminum of 4 mm thickness. Geometry and dimensions are shown in Figure 6. System identification parameters are given in Table 2.

An estimate for the system matrix A is first obtained using a scattered subset of the spatial frequency samples. The locations of subset points are shown in Figure 6. Equation (17) is solved to identify the mode shapes and feed-through function. The normalized mode shapes and feed-through function are plotted in Figures 4 and 5. Due to the difficulties in visualizing a four dimensional quantity, we evaluate model quality by taking a planar section of the spatial frequency response. An elevation of the section is shown in Figure 6. The measured, identified model, and error system frequency responses evaluated along the section are shown in Figures 7 (a), (b), (c) respectively.

Frequency Range	10-100 (Hz)
Eqi-distance F Samples	577
Number of Spatial Samples	468
Spatial Sampling interval	2.63 cm
Excitation	Colored Chirp

Table 2: Plate system identification parameters

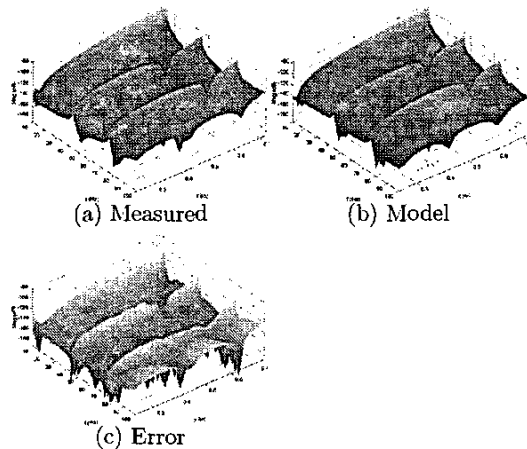


Figure 7:

5 Conclusions

A technique has been presented for identifying a class of distributed parameter systems from a set of spatially distributed frequency responses. The systems are modelled as a finite sum of second order transfer functions with spatially variant numerators and feed-through.

In an attempt to evenly distribute model error, the identification is cast as a single-input multi-output identification problem. An estimate for the system dynamics is sought using a frequency domain subspace algorithm. Samples of the mode shapes and feed-through function are first identified then used to reconstruct the continuous functions. If the spatial Fourier transform is known, the error due to under sampling can be quantified.

Experimental identification of a simply supported beam and cantilever plate has shown an adequate correlation in the frequency domain between the measured system and identified model. In both cases the majority of discrepancy is due to small errors in the resonant frequencies. Current work involves the development of an efficient optimization algorithm to minimize such errors.

Other topics of current research include: the automatic identification of non-distributed dynamics $H(s)$, experimental identification incorporating piezoelectric sensor voltages, time domain identification techniques, and stochastic analysis.

References

- [1] D. Halim and S. O. R. Moheimani, "Experiments in spatial H_∞ control of a piezoelectric laminate beam," in *Perspectives in Robust Control* (S. O. R. Moheimani, ed.), ch. 8, pp. 104–121, Springer-Verlag, 2001.
- [2] S. Skogestad and I. Postlethwaite, *Multivariable Feedback Control*. John Wiley and Sons, 1996.
- [3] K. Zhou, J. C. Doyle, and K. Glover, *Robust and Optimal Control*. Upper Saddle River, N.J.: Prentice Hall, 1996.
- [4] S. O. R. Moheimani, "Broadband disturbance attenuation over an entire beam," *Journal of Sound and Vibration*, vol. 227, no. 4, pp. 807–832, 1999.
- [5] D. Halim and S. O. R. Moheimani, "Spatial resonant control of flexible structures - application to a piezoelectric laminate beam," *IEEE Transactions on Control System Technology*, vol. 9, pp. 37–53, January 2001.
- [6] D. Halim and S. O. R. Moheimani, "Spatial H_2 control of a piezoelectric laminate beam: Experimental implementation," *IEEE Transactions on Control Systems Technology*, vol. 10, pp. 533–546, July 2002.
- [7] L. Meirovitch, *Elements of Vibration Analysis*. Sydney: McGraw-Hill, 2nd ed., 1996.
- [8] A. R. Fraser and R. W. Daniel, *Perturbation Techniques for Flexible Manipulators*. Kluwer Academic Publishers, 1991.
- [9] J. Heng, J. C. Akers, R. Venugopal, M. Lee, A. G. Sparks, P. D. Washabaugh, and D. Bernstien, "Modelling, identification, and feedback control of noise in an acoustic duct," *IEEE Transactions on Control Systems Technology*, vol. 4, no. 3, pp. 283–291, 1996.
- [10] R. D. Cook, *Finite Element Modelling for Stress Analysis*. John Wiley and Sons, 1995.
- [11] Y.-H. Lim, V. V. Varadan, and V. K. Varadan, "Closed-loop finite element modelling of active/passive damping in structural vibration control," in *Proc. SPIE Smart Materials and Structures, Mathematics and Control in Smart Structures, SPIE Vol. 3039*, (San Diego, CA), March 1997.
- [12] D. J. Ewins, "Modal testing as an aid to vibration analysis," in *Proc. Conference on Mechanical Engineering*, May 1990.
- [13] N. M. M. Maia and J. M. M. e Silva, eds., *Theoretical and Experimental Modal Analysis*. Hertfordshire, England: Research Studies Press, 1997.
- [14] S. O. R. Moheimani, "Minimizing the effect of out-of-bandwidth dynamics in the models of reverberant systems that arise in modal analysis: Implications on spatial H_∞ control," *Automatica*, vol. 36, pp. 1023–1031, 2000.
- [15] P. Lancaster and K. Salkauskas, *Curve and Surface Fitting*. Academic Press, 1986.
- [16] M. Unser, "Splines, a perfect fit for signal and image processing," *IEEE Signal Processing Magazine*, vol. 16, pp. 22–38, November 1999.
- [17] M. Unser, A. Aldroubi, and M. Eden, "Polynomial spline signal approximations: Filter design and asymptotic equivalence with shannon's sampling theorem," *IEEE Transactions on Information Theory*, vol. 38, pp. 95–103, January 1992.
- [18] R. Hummel, "Sampling for spline reconstruction," *SIAM Journal of Applied Mathematics*, vol. 43, pp. 278–288, April 1983.
- [19] T. Blu and M. Unser, "Quantitative fourier analysis of approximation techniques: Part 1 - interpolators and projectors," *IEEE Transactions on Signal Processing*, vol. 47, pp. 2783–2795, October 1999.
- [20] R. L. Fante, *Signal Analysis and Estimation. An Introduction*. John Wiley and Sons, 1988.
- [21] T. McKelvey, A. J. Fleming, and S. O. R. Moheimani, "Subspace based system identification for an acoustic enclosure," *ASME Journal of Vibration and Acoustics*, vol. 124, pp. 414–419, July 2002.
- [22] K. Liu, R. N. Jacques, and D. W. Miller, "Frequency domain structural system identification by observability range space extraction," in *Proc. American Control Conference, Vol. 1*. (Baltimore, MD), pp. 107–111, June 1994.
- [23] T. McKelvey, H. Akcay, and L. Ljung, "Subspace based multivariable system identification from frequency response data," *IEEE Transactions on Automatic Control*, vol. 41, pp. 960–978, July 1996.
- [24] A. J. Fleming, S. Behrens, and S. O. R. Moheimani, "Optimization and implementation of multi-mode piezoelectric shunt damping systems," *IEEE/ASME Transactions on Mechatronics*, vol. 7, pp. 87–94, March 2002.